Modeling the formation of ordered nano-assemblies comprised by dendrimers and linear polyelectrolytes: The role of Coulombic interactions

E. Eleftheriou and K. Karatasos

Citation: J. Chem. Phys. **137**, 144905 (2012); doi: 10.1063/1.4757666
View online: http://dx.doi.org/10.1063/1.4757666
View Table of Contents: http://jcp.aip.org/resource/1/JCPSA6/v137/i14
Published by the American Institute of Physics.

Additional information on J. Chem. Phys.

Journal Homepage: http://jcp.aip.org/
Journal Information: http://jcp.aip.org/about/about_the_journal
Top downloads: http://jcp.aip.org/features/most_downloaded
Information for Authors: http://jcp.aip.org/authors

ADVERTISEMENT

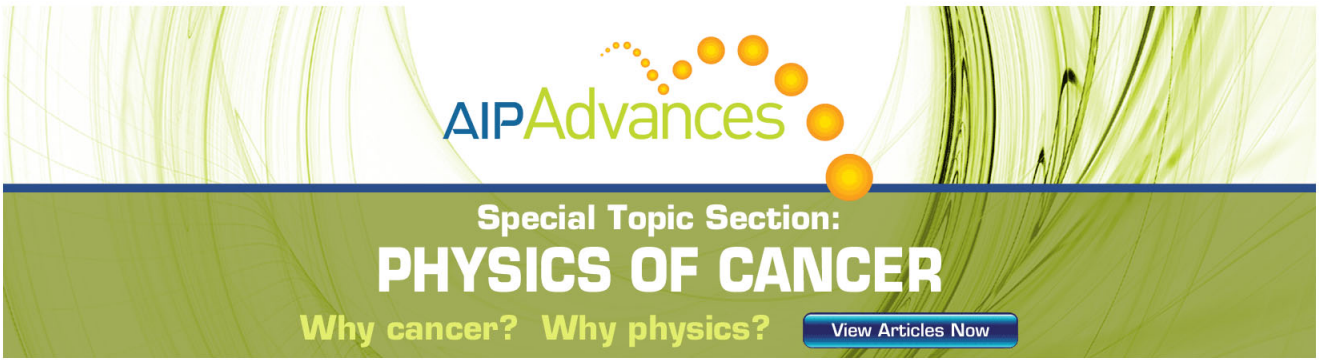

Modeling the formation of ordered nano-assemblies comprised by dendrimers and linear polyelectrolytes: The role of Coulombic interactions

E. Eleftheriou and K. Karatasos[a)]
Physical Chemistry Laboratory, Chemical Engineering Department, Aristotle University of Thessaloniki, 54124 Thessaloniki, Greece

(Received 9 July 2012; accepted 20 September 2012; published online 11 October 2012)

Models of mixtures of peripherally charged dendrimers with oppositely charged linear polyelectrolytes in the presence of explicit solvent are studied by means of molecular dynamics simulations. Under the influence of varying strength of electrostatic interactions, these systems appear to form dynamically arrested film-like interconnected structures in the polymer-rich phase. Acting like a pseudo-thermodynamic inverse temperature, the increase of the strength of the Coulombic interactions drive the polymeric constituents of the mixture to a gradual dynamic freezing-in. The timescale of the average density fluctuations of the formed complexes initially increases in the weak electrostatic regime reaching a finite limit as the strength of electrostatic interactions grow. Although the models are overall electrically neutral, during this process the dendrimer/linear complexes develop a polar character with an excess charge mainly close to the periphery of the dendrimers. The morphological characteristics of the resulted pattern are found to depend on the size of the polymer chains on account of the distinct conformational features assumed by the complexed linear polyelectrolytes of different length. In addition, the length of the polymer chain appears to affect the dynamics of the counterions, thus affecting the ionic transport properties of the system. It appears, therefore, that the strength of electrostatic interactions together with the length of the linear polyelectrolytes are parameters to which these systems are particularly responsive, offering thus the possibility for a better control of the resulted structure and the electric properties of these soft-colloidal systems.
© *2012 American Institute of Physics*. [http://dx.doi.org/10.1063/1.4757666]

I. INTRODUCTION

Mixtures of linear polymers and colloidal particles are one of the most promising routes towards the formation of composite materials in which advantageous features of both components can be combined and exploited in technologically advanced applications.[1–3] In neutral systems, chemistry and structural features like the size (or the size polydispersity) of the colloidal particles,[4] the molecular weight and the flexibility of the linear polymer,[5–7] and the polymer/particle stoichiometry[8,9] are key parameters which determine the morphology and the physical properties of the mixture. In case that one or both of the components are electrically charged, apart from the aforementioned factors, fine-tuning of their physicochemical properties can be facilitated by properly manipulating additional parameters which affect the interplay between the electrostatic and the depletion forces among the two components, such as the density and the sign of the charge of each constituent and the ionic strength of the dispersion.[6,10–12]

The most interesting feature of such polymer/colloid interpolyelectrolyte complexes (IPECs) is their ability to respond to external stimuli such as pH, ionic strength, and application of an external electric field.[10,12–16] The responsiveness of IPECs in controlled environmental changes is among the most desired properties when it comes to their utilization as "smart" materials in industrial applications such as in sensors, in coatings, in molecular-separation technologies, in gel electrophoresis, and in biomedicine.[1,17,18] The ability of these systems to alter their properties upon modification of the microenvironmental conditions is significantly enhanced when the colloidal component behaves as a soft rather than as a hard particulate.[16,19,20] In this case, the propensity of the soft particle to swell/collapse upon a creation of an osmotic gradient between its interior and the exterior environment, may result in a prominent change of its dimensions and thus in the structural characteristics of the IPEC it participates in. This utility of colloidal dispersions based on soft particles, has triggered an increasing scientific interest on such systems particularly in the last decade.[9,21,22]

Among the categories of soft particles utilized for the formation of polymer/colloidal mixtures, star molecules,[9,23] branched[24,25] and hyperbranched polymers,[10,26–28] were recently placed under the focus of the scientific community. Such systems were found to be of particular significance not only due to their enhanced responsiveness, but also because of their nanosized dimensions (i.e., from 100 nm down to 1 nm), which opened new perspectives for a wide range of novel applications, including targeted drug delivery and gene-based therapy.[29,30] Attributes like the large surface to volume ratio, the multifunctionality and the distinct features of their internal structure, rendered nanogels based on these soft polymeric

a)Author to whom correspondence should be addressed. Electronic mail: karatas@eng.auth.gr.

 © 2012 American Institute of Physics

particles particularly effective for nanomedical uses.[31–34] One category of polymers which are considered among the most promising candidates as the soft-colloidal component for the formation of IPECs (and thus for the fabrication of responsive nanogels) with molecules of biological interest, are the hyperbranched polymers characterized by a regularly branched pattern known as dendrimers.[32,35,36] Several families of these molecules have been found appropriate for biomedical applications since they combine all the aforementioned desirable characteristics (nanosized dimensions, high responsiveness due to their ionizable groups, multivalency which enhances bioconjugation leading to higher exchange rates) with favorable mechanical properties and low toxicity levels which promotes bioavailability.[37–39] Specifically, those with a cationic surface have been successfully utilized in the development of efficient non-viral binding agents and vectors for oligonucleotide delivery.[40–44]

The aim of the present study is to explore generic effects in the formation of nano-assemblies comprised by charged dendrimer molecules and linear polyelectrolytes (LPE) of opposite charge, using as stimulus the variation of the strength of electrostatic interactions. These mixtures can be considered as models for actual systems formed by surface-ionizable cationic dendrimers and negatively charged linear polyelectrolytes.[16,45–47] To check the effects of the length of the linear component in the characteristics of the formed IPECs and consequently of the entire system, we explored two distinctly different sizes of the linear polyelectrolyte. In all cases, the systems remain overall electrically neutral.

Apart from monitoring the structural changes in the complexes induced by the variation in the electrostatic strength and the length of the linear chain, we also explored certain aspects of the dynamic response of the different constituents, which provided a more concise picture on the role of the individual components to the observed behavior. Although formation of IPECs between charged multibranched polymers and linear polyelectrolytes has been previously explored by means of computer simulation techniques,[48–54] to our knowledge this is the first simulation study which considers a multidendrimer/multichain system with the dendrimers and the linear chains bearing all the common internal degrees of freedom (bond stretching, angle bending, and torsion rotation), with explicit presence of counterions and solvent molecules in which complexation and ordering within the formed complexes can be examined in more detail.

II. SYSTEMS' DESCRIPTION AND SIMULATION DETAILS

We have modeled two systems referred to as S1 and S2, as described in Table I. For both the examined systems, the concentration is kept well below the corresponding overlap concentration of the polymeric components (see Figure S1 in the supplementary material[55] for a picture of the constructed models), while the overall volume fraction (considering each monomer, counterion and solvent bead as a sphere represented by its Van der Waals (VDW) radius) remains lower than the random close packing limit.

TABLE I. Details on the composition of the simulated systems.

System code	S1	S2
Number of dendrimer molecules	30	30
Dendrimer generation	3	3
Charge per dendrimer	+24	+24
Number of linear chains	30	15
Monomers per linear chain	24	48
Charge per linear chain	−24	−48
Number of positive counterions	720	720
Number of negative counterions	720	720
Number of solvent beads	1544	1544
Vol. fraction of dendrimers	0.07	0.07
Vol. fraction of linear chains	0.05	0.05
Total volume fraction	0.33	0.33

For the monomers of the polymeric species as well as for the counterions and the solvent beads, we have adopted a bead-spring representation (with flexible bonds), as in our previous works.[56–58] The dendrimer molecules were modeled with a trifunctional core and a bifunctional branching pattern (see Figure S2 in the supplementary material[55]), which was grown up to the 3rd generation. According to this branching pattern each dendrimer was comprised by 91 monomers, 24 of which (those located at the outer generational shell) were assigned a charge of +1, while each monomer (of unit length) of a linear chain was oppositely charged. A number of 720 positive and 720 negative monovalent counterions (represented as spherical beads identical to the charged polymeric monomers) were included as well, so that the systems remained electrically neutral.

The set of parameters which described the different energetic contributions was based on the DREIDING forcefield[59] and included all the common internal degrees of freedom (i.e., bond stretching, angle bending, and torsions) as well as intra- and intermolecular non-bonded terms according to the Lennard-Jones (for the uncharged beads) and to the Weeks-Chandler-Anderson[60] (for the charged beads) potentials. Parameterization of dendrimer systems with the aforementioned set of parameters has been widely employed for the representation of united-atom models.[61–63] Electrostatic interactions were estimated using full Ewald summation to account for the periodic boundary conditions. The simulations were performed in the constant volume–constant temperature (*NVT*) ensemble. The simulation protocol followed involved energy minimization and MD cycles for equilibration of the structures prior to the production runs. The set of energetic parameters used and the steps of the simulation protocol followed, are the same as those described in Ref. 56. All the lengths are measured in units of the parameter σ of the non-bonded potential between two charged beads, while time is expressed in terms of the characteristic time of the model τ, which corresponds to approximately 1.2×10^3 MD steps. After equilibration, trajectories of 6×10^3 τ were generated and snapshots were saved with a frequency of 0.85 τ.

For comparison purposes to relevant results of previous works where charged models of hyperbranched molecules were studied,[56,64–66] the intensity of the electrostatic interactions was modulated by means of varying the Bjerrum length

(l_B), which is related to the Debye screening length κ^{-1} by

$$\kappa^{-1} = \frac{1}{\sqrt{4\pi l_B \sum_i c_i z_i^2}}. \quad (1)$$

In Eq. (1), c_i and z_i are the concentration and the valence of ith species of ions in the solution, respectively. The range of Bjerrum lengths explored in our study extended from $l_B/\sigma = 1$ to $l_B/\sigma = 10$ which would translate to real units[56,66] of approximately 0.37 nm–3.7 nm (for comparison, the Bjerrum length of water at ambient temperature is close to 0.7 nm which would correspond to $l_B/\sigma \cong 2$ in our model). In experimental conditions, low electrostatic levels could be realized in polar solvents and in conditions of highly screened Coulombic interactions, while intermediate or strong electrostatic levels (with Bjerrum lengths of the order of 10 nm or larger) could be attained upon mixing low polarity organic solvents or in polar/non-polar co-solvent mixtures.[67–69] In such cases, solubilisation of dendrimers could be accomplished by their appropriate functionalization.[70,71] An alternate route for the modulation of the strength of electrostatic interactions would be by changing temperature and/or the level of electrostatic screening, e.g., by varying the ionic strength of the solution.[65,72,73]

III. STRUCTURAL AND MORPHOLOGICAL CHARACTERIZATION

Starting from the weak electrostatic regime and by increasing the strength of electrostatic interactions, it is expected that the interplay between energetic and entropic factors may affect the phase behavior of the mixture[74] while at the same time leading to distinct morphological characteristics of the formed complexes.[10] Before examining the resulted equilibrium morphologies assumed by the two systems, it is informative to follow the structural response at the molecular level.

In previous computational studies where the behavior of charged dendrimers was studied under a varying strength of electrostatic interactions,[56,65,66,75] a non-monotonous dependence of their average size was noted when passing from the weak to the strong electrostatic regime. A rather monotonous dependence with a tendency towards lower values as l_B was increasing, was found for the average size of single non-regularly branched polymers in 1:1 stoichiometric complexes with a neutralizing LPE,[64] with those closer to a dendrimer topology exhibiting a weaker dependence. Figure 1 depicts the average size of the dendritic and the linear components as a function of the strength of the Coulombic interactions. As can be readily inferred, the average size of the two components remains practically unaffected by the changes in Bjerrum length.

The size of the dendritic molecules does not exhibit the non-monotonous dependence on l_B quoted above for the systems comprised solely by dendrimers. The linear components assume average sizes larger by about 20% and 80% in S1 and S2, respectively, compared to the dendrimer molecules, while the relative difference in their dimensions cannot be accounted for either by that expected for fully stretched chains

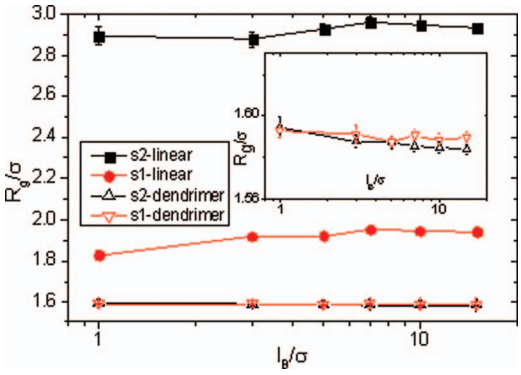

FIG. 1. Average radius of gyration of the dendritic and the linear components of the mixture. The inset shows the radius of gyration of the dendrimers in a more detailed scale.

or by that of Gaussian coils. Indeed, when examining the ratio of the average squared end-to-end vector over the average squared radius of gyration $\langle R_{ee}^2 \rangle / \langle R_g^2 \rangle$ for the linear chains (see Figure S3 in the supplementary material[55]) it appears that the half-length polyelectrolyte molecules assume on average a more stretched shape compared to their double-length analogues. Such differences can be rationalized by the competition mainly between the electrostatic forces and the cost in bending energy,[10] which may result in a plethora of distinctly different conformations of the linear chain.[51–53] Particularly in our case where many dendrimers and LPEs are present, a larger number of different configurations of the linear chains can be realized. The type and the relative probability of appearance of the different conformations of the LPEs could thus be affected by the strength of Coulombic interactions.

To obtain a more detailed account on the dependence of the conformational characteristics of the LPEs on the intensity of electrostatic interactions, we have monitored the distributions of the end-to-end vector of the chains as shown in Figure 2. A visual inspection of the distributions shows that for both systems the increase in the strength of electrostatic interactions induces significant changes. In the stoichiometric system (S1) and in the weak electrostatic regime (i.e., low l_B values), the distributions appear asymmetrical towards larger distances (i.e., extended conformations). As the Coulombic interactions grow stronger the distributions become broader while short end-to-end distances also appear. The analogous changes in the distributions of the non-stoichiometric system (S2) are more drastic. Increase of the electrostatic strength triggers the appearance of several peaks which grow in number as l_B becomes higher. The peaks corresponding to the extreme distances in both systems, are consistent with the existence of "U-shaped" conformations where the two ends of the chain come to a close proximity and to extended conformations where the LPEs play the role of a "linker" between one or more of the dendrimers.[51,52] The intermediate distances denote the presence of different combinations. An impression of the realization of such conformations is shown in Figure S4 in the supplementary material[55] where a snapshot is depicted at $l_B/\sigma = 10$ for the two systems. For the stoichiometric system S1, "U"-shaped, "L"-shaped, and fully extended conformations are present. For the non-stoichiometric

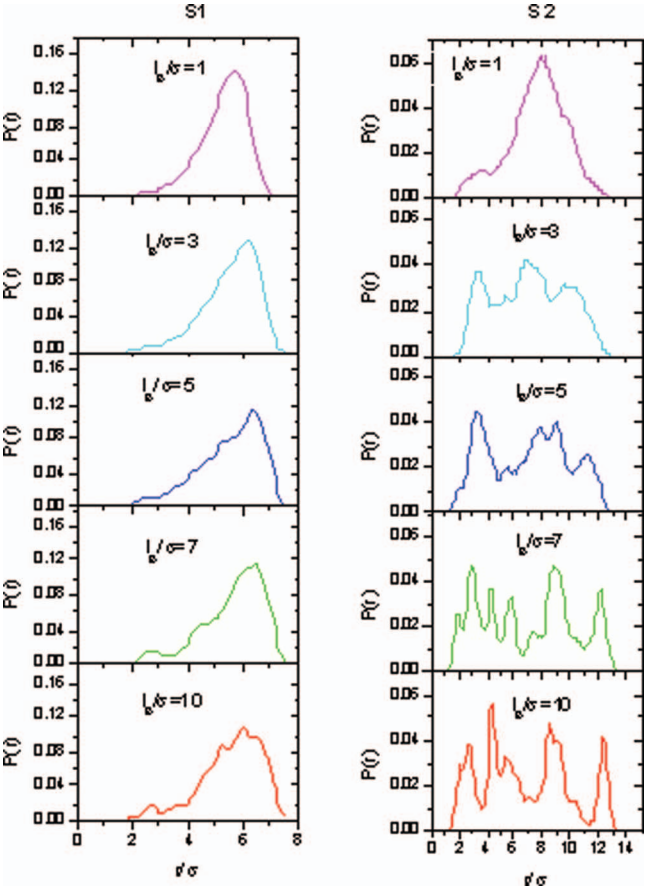

FIG. 2. Probability distributions of the end-to-end distance of the linear polyelectrolytes in the system with short (S1, left) and long (S2, right) chains.

system (S2), "U"-shaped, "U-tail" as well as extended conformations can be discerned. Apart from the "U"-shaped conformations, those where the chains are fully or partly extended, act as "binders" between neighboring dendrimers stabilizing the structure.

The distinct conformations realized by the LPEs in the two systems affect their relative packing in the solution as shown in Figure 3, where the intermolecular monomer-monomer radial distribution functions for the linear chains are plotted. At low l_B values the pair correlation functions show a distinct maximum corresponding to a separation very close to twice the radius of gyration of the dendrimer molecule, implying that the different linear chains remain relatively far apart, separated by the dendrimer molecules.

As the strength of electrostatic interactions grows, the main peak shifts to lower separations, while at higher values of Bjerrum length additional "shoulders" or even well defined maxima appear, both at lower and at higher separations. The lower separation peak close to a distance of 2σ, would be consistent with the intervention either of solvent beads or counterions between neighboring chains, but its appearance only at the higher l_B values indicates that the counterion intervention is the more probable reason. The appearance of the peaks at larger separations could be attributed to similar reasons, if we envisage the intervention of counterion layers (i.e., condensed counterions) between the dendritic molecules and the linear polyelectrolytes.

To check this argument we have examined the profiles of interpenetration between the dendrimer molecules and the rest of the components as well as the pair correlation functions between charged monomers and counterions (see Figures S5 and S6 in the supplementary material[55]). Our findings show that for both systems increase of the level of the Coulombic interactions incurs the localization of the LPE close to the dendritic periphery where the majority of the charged dendrimer beads are located. In addition, a much more drastic enhancement of the degree of ionic pairing between the monomers of the linear chain and those of the dendrimer is observed, as compared to that between the polymeric species and the corresponding counterions. This behavior arises from the fact that the entropic gain is higher when the counterions remain less localized.[28,76,77] The more effective physical adsorption of the LPEs on the dendrimer surface and the rearrangement of the counterions close to the dendrimer periphery upon increase of the strength of Coulombic interactions, results in the formation of a modulating charge profile across the dendritic structure as shown in Figure 4. The behavior of the effective charge profiles in the two systems are qualitatively very similar. The positive peaks close to the dendrimer's radius of gyration arise mainly from the backfolding of the positively charged dendrimer monomers as can be inferred upon inspecting the corresponding monomer profiles (see Figure S5 in the supplementary material[55]). The negatively signed minima which deepen as Bjerrum length increases are a direct

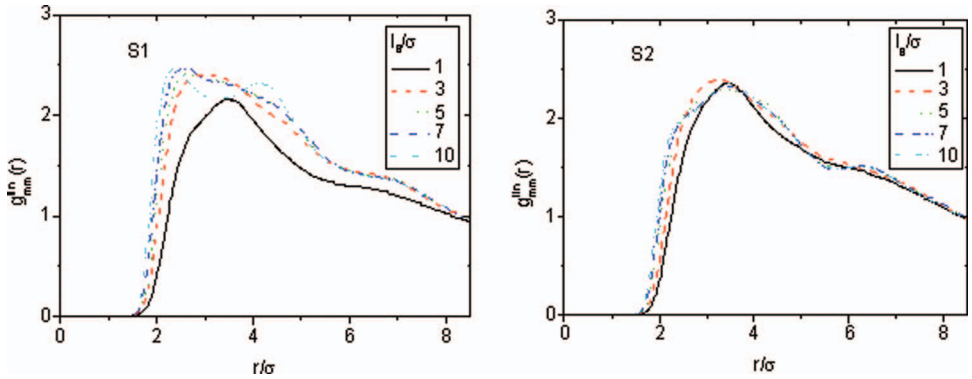

FIG. 3. Monomer-monomer intermolecular pair correlation functions of the linear chains at different values of Bjerrum length for the stoichiometric (left) and the non-stoichiometric (right) model.

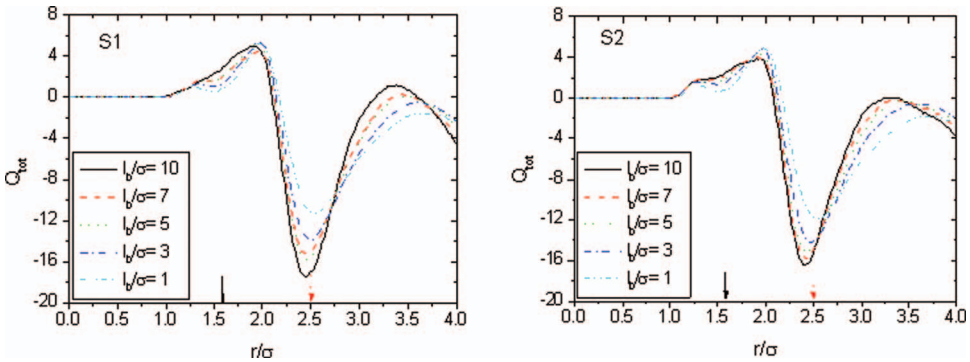

FIG. 4. Average effective charge profiles with respect to the center of mass of the dendrimer molecules for the examined systems. The solid arrow marks the location of the dendrimer's radius of gyration while the dotted arrow denotes the spatial extent of the dendrimer's periphery. For the calculation of the profiles, all charged monomers and counterions in the vicinity of each dendrimer have been taken into account.

effect of the LPEs physical binding, that is, their increasing localization near the dendrimers' surface as quoted above.

It is noteworthy that for both systems the location of the negative minimum in the charge profiles appears rather insensitive to Bjerrum length variations; it is shifted only by approximately 5% closer a distance from the dendrimer's center of mass when passing from the weak to the stronger electrostatic regime. Since the main contribution of the negative charge to the effective profiles arises from that of the linear chains (see Figure S5 in the supplementary material[55]), the aforementioned behavior can be ascribed to the action of the close-range excluded volume interactions between the LPEs' and the dendrimers' beads which allows only for a very small additional approaching between the oppositely charged monomers as l_B increases.

The observed effective "charge reversal" of the complexes close to the dendrimers' periphery is a manifestation of the so-called overcharging phenomenon which has been predicted theoretically,[78,79] observed experimentally[80,81] and seen in previous pertinent simulation studies.[64,82,83] As in the case of colloidal/linear polyelectrolyte systems, in mixtures of charged dendrimers and oppositely charged linear polyelectrolytes overcharging has been found to play a key role in the ability of the formed complexes to self-organize in supramolecular assemblies.[13,84,85] Attributes like the effective surface charge density of the colloidal particles (here the dendrimers), the molecular weight and the concentration of the two components, may affect decisively the characteristics of the resulted structures.[10,26,84]

In the case of the systems simulated in this work, self-assembly of the complexes driven by changes in the strength of electrostatic interactions is also observed. Figures 5 and 6 present the morphological changes of the examined systems upon increase of Bjerrum length. Already from low Bjerrum length values, significant composition heterogeneities are formed, which, upon increasing the strength of electrostatic interactions appear to be enhanced leading to polymer-rich and solvent/counterion-rich regions. Evidently, in both systems formation of interconnected film-like structures takes place within the polymer-rich phase.

The morphological characteristics of the resulted structure in the complexes differentiate between the stoichiometric (S1) and the non-stoichiometric models (S2) as can be identified upon inspecting the snapshots and by examining the relevant static structure factors (see Figure S8 in the supplementary material[55]). The differences in the structures assumed by S1 and S2 become significant only at lengthscales comparable to, or shorter than the size of a dendrimer. At longer distances both systems exhibit a similar behavior characterized by the first neighbor peak and a well-defined maximum at low-q limit which signifies the existence of a stable supramolecular structure within the polymer-rich region.

Although in polyelectrolyte solutions the size of the linear chains and their stiffness (among other factors) are known to play a significant role in self-organization phenomena,[7,86] it is not straightforward to predict the relative importance of each energetic/entropic contribution to such a process, particularly when it comes to complex polymeric systems with many degrees of freedom as those examined in this work. We may however obtain a qualitative picture as to the main driving force responsible for the observed differences between the examined systems, by calculating separately the different contributions to the excess osmotic coefficient according to Eq. (2)[87]

$$\frac{\pi}{\rho k_B T} - 1 = \frac{\pi_{Bond}}{\rho k_B T} + \frac{\pi_{VDW}}{\rho k_B T} + \frac{\pi_{Elec}}{\rho k_B T}. \qquad (2)$$

In Eq. (2), π is the osmotic pressure, ρ is the solution number density, while the rest of the terms correspond to contributions arising from bonded, Van der Waals and electrostatic interactions that are present in each system.

Figure 7 shows the different contributions to the excess osmotic pressure as a function of Bjerrum length. A cursory glance at Figure 7 shows that the more significant contributions to the excess osmotic coefficient originate from the electrostatic and the VDW interactions. Interestingly though, the main difference between the two systems arises from the VDW contribution (note that the electrostatic contributions are nearly identical for the two examined systems). Taking into account the distinct conformational features of the LPE components in the two systems (Figure 2) and the differences noted in the relative spatial arrangement of their monomers (Figure S5), both of which influence the short-range intra- and intermolecular VDW interactions involving LPE monomers, it can be concluded that the length of LPE chains plays a key

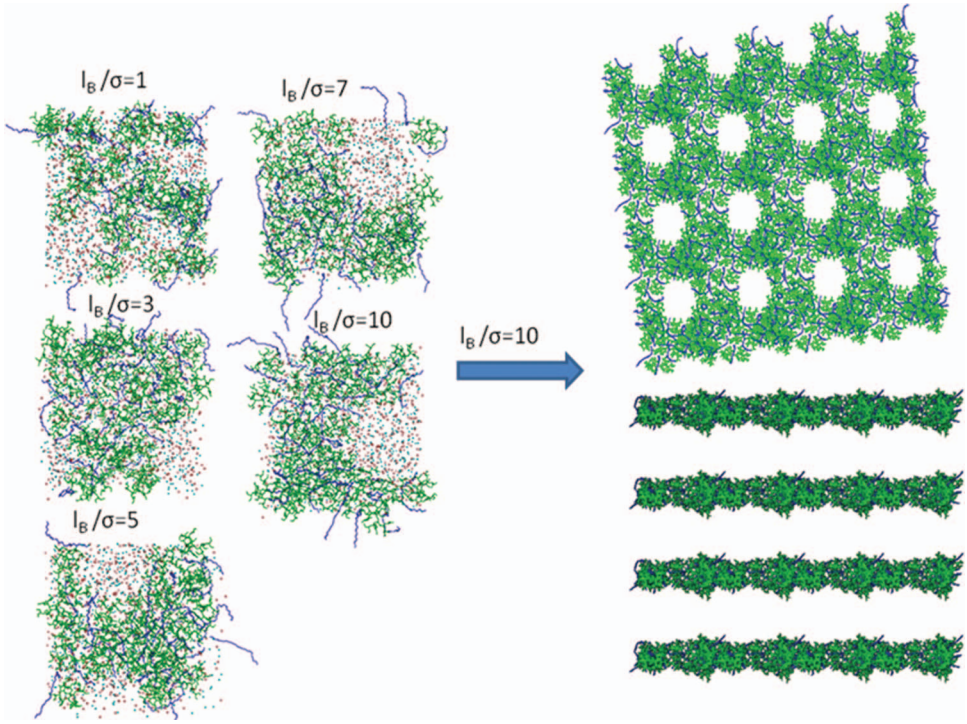

FIG. 5. (Left side of the arrow) Snapshots of the system comprised by dendrimers and short LPEs (S1) at different Bjerrum lengths (solvent beads are omitted for clarity). (Right side of the arrow) The simulation box at $l_B/\sigma = 10$ together with periodic neighboring cells, in frontal (up) and side (below) view (counterions and solvent beads are omitted for clarity).

role in the differences observed in the thermodynamics of the two systems, and therefore in their final morphologies.

Apart from the aforementioned disparities though, between S1 and S2 models, an intriguing result is the formation of a flattened structure in contrast to the three-dimensional random close packing or qubic-lattice morphologies that have been observed in charged dendrimer solutions[56,88] or charged colloidal systems.[67] Similar self-assembly of dendrimers in film-like structures, however, have been observed experimentally in the presence of substrates.[14,85,89] More specifically, composites of cationic dendrimers with linear anionic polymers were found to form well-defined two-dimensional

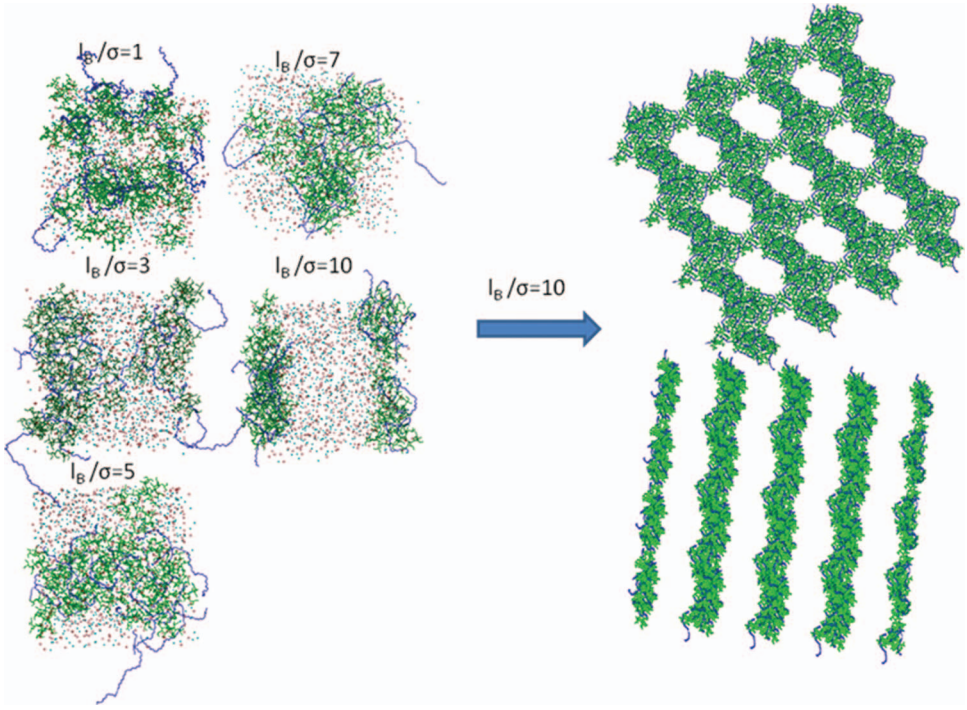

FIG. 6. The analogous of Figure 5, but for the system comprised by dendrimers and the longer LPEs (S2).

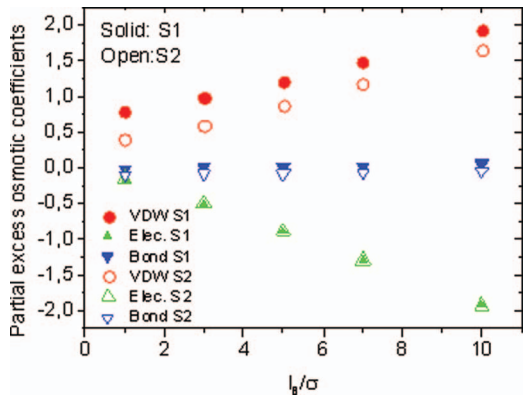

FIG. 7. Contributions to the excess osmotic coefficient arising from bonded, Van der Waals, and electrostatic interactions.

structures, the features of which (i.e., thickness, stability) could be regulated by changing the overall charge (e.g., by ionizing the peripheral only or both, the peripheral and the internal ionizable groups) of the dendritic component.[14,84,85] Under the examined conditions of dendrimer size and charging pattern, our systems appear to form films of thickness comparable to two dendrimer diameters (i.e., in actual units of approximately 2 nm). This finding, combined with those of previous studies[10,26,58] implies that under appropriate changes in factors such as the dendrimer size, their charging density, and the length of the linear polyelectrolytes, the characteristics of the resulted morphology in the polymer-rich region might be controlled down to the nanoscale.

IV. DYNAMIC RESPONSE

Previous studies in colloidal systems[68,90,91] and in dendrimer polyelectrolyte solutions[58,92] revealed that the dynamic response of such systems to changes in thermodynamic parameters of their microenvironment, affect decisively the characteristics of the final (equilibrium or non-equilibrium) morphology. The degrees of freedom available to the colloidal particles, the nature of the effective interactions between them and the existence of spatial or thermodynamic constraints[90,91,93] essentially dictate the dynamic modes of the structural relaxation of the individual particulates or of their self-assemblies,[93–95] driving thus these systems to states such as glass transition, gelation or to other arrested states.[96–99]

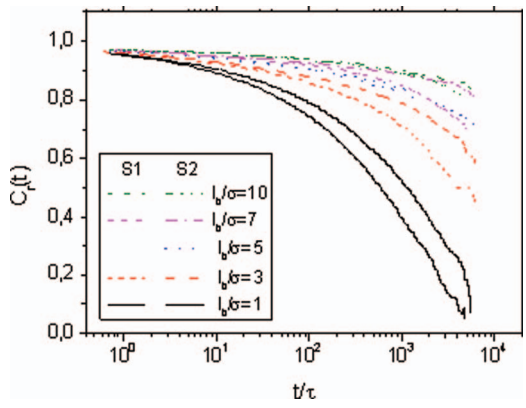

FIG. 8. Overall dendrimer reorientational correlation functions for varying strengths of electrostatic interactions. Thin lines correspond to the S1 and thick lines to the S2 model.

Systems comprised solely by dendritic components similar to those of the present study were found to exhibit a characteristic slow-down of their molecular-scale dynamics upon increase of the strength of electrostatic interactions, resembling that observed when approaching a colloidal glass transition.[58,75] The gradual freezing-in of translational and rotational degrees of freedom, however, was realized only at the strong electrostatic regime, i.e., at $l_B/\sigma \geq 10$. To compare this behavior to the analogous dynamic response of the dendritic components of our systems at the molecular-level, we have monitored the orientational relaxation function

$$C_r(t) = \langle \hat{g}(t)\hat{g}(0)\rangle, \tag{3}$$

where $\hat{g}$ represents unit vectors connecting the center of mass of a dendrimer to the monomers belonging to its outer generational shell. The averaging is performed over all such unit vectors of a dendrimer and over all the dendrimer molecules. This function is sensitive to the overall dendrimer rerorientational motion.[100]

Figure 8 shows the $C_r(t)$ spectra for the different Bjerrum length and for both of the examined models. As evidenced by the decreasing degree of decorrelation of the $C_r(t)$ spectra upon increasing l_B, dendrimer molecules undergo a gradual slow-down of their rotational motion in both the examined systems. In addition, the dendrimers' rotational motion is slower in the system consisted of the longer LPE chains within the entire range of the examined l_B values. This notion marks a clear difference with respect to the behavior observed in the charged dendrimer solutions without the presence of the LPEs. In particular, the obstruction of the overall dendrimer reorientation in the present systems is manifested already within the weak electrostatic regime (i.e., at l_B/σ well below 10) as a result of the thermodynamically preferable complexation of the dendrimer molecules with LPEs, even at relatively low electrostatic levels (see Figure 4 and Figures S5 and S6 in the supplementary material[55]). This observation is to be contrasted to the behavior found in systems comprised solely by charged dendrimers,[56,58] where the charge reversal responsible for the effective like-charge attraction between dendrimer molecules takes place only in the regime of strong electrostatic interactions.

The fact that in the non-stoichiometric system (i.e., in S2 with LPE/dendrimer size ratio of ∼1.8) dendrimer reorientation is slower compared to that observed in the stoichiometric model (i.e., in S1, with LPE/dendrimer size ratio of ∼1.2) should be attributed to the realization of different conformational states of the longer linear component which may affect the interconnectivity between the formed complexes. Namely, the ability of the longer LPE polymer to assume conformations which may result to a physical link between a larger number of dendrimer molecules (Figure 2, and Figure S4[55]), as well as the spatial constrictions and the energetic cost involved in the reorientation of dendrimer when

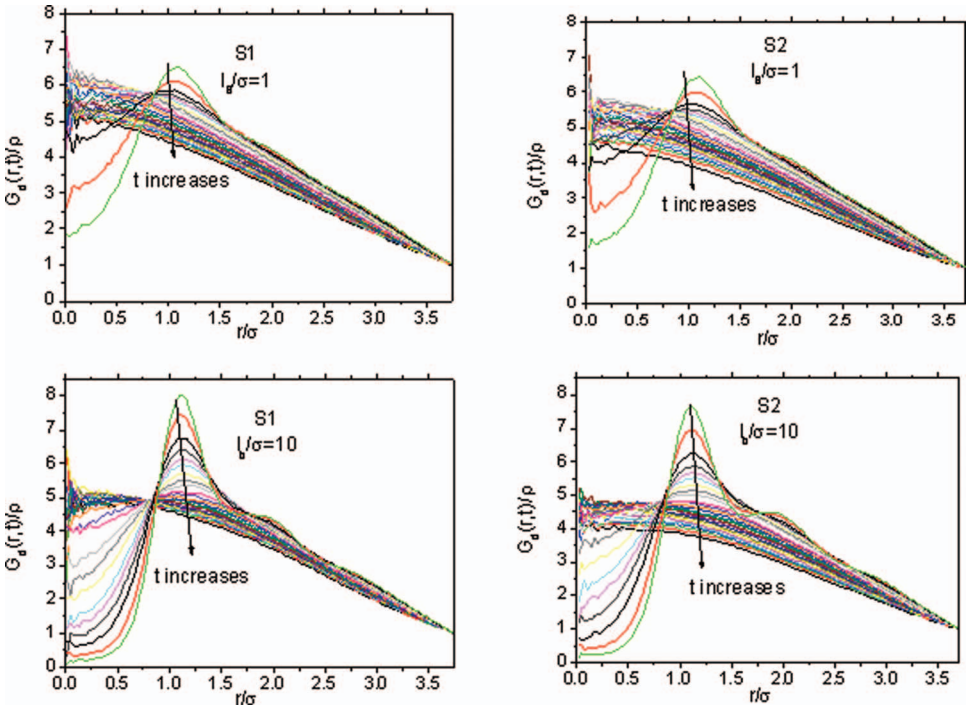

FIG. 9. Distinct Van Hove space-time correlation functions arising from the centers of mass of the dendrimer molecules, for the lower ($l_B/\sigma = 1$) and the higher ($l_B/\sigma = 10$) Bjerrum lengths examined, for the system with the short (S1) and the long (S2) LPE chains. The different curves correspond to time separations t between 0 and 1025τ. The arrows point to the direction of increasing t.

a longer chain is physically bound to it, can account for the observed behavior.

An analogous slowing-down of the individual diffusive motion of the dendrimer molecules as the strength of electrostatic interactions increases, is also observed in the presently examined systems (see Figure S9 in the supplementary material[55]). In other words, both, individual rotational as well as translational motion of the soft-colloidal components of the mixtures, points towards a kinetic arrest of the complexes as the intensity of Coulombic interactions grows. Moreover, the route towards this dynamic slow-down and the features of the final morphology assumed by the complexes can be also affected by the characteristics of their collective motion, much in analogy to the behavior observed in dynamically arrested colloidal systems.[101,102] To probe the synergistic motion of the complexes upon increasing the strength of Coulombic interactions, we have monitored the distinct Van Hove space-time function of the centers of mass of the dendrimer molecules $G_d(t)$

$$G_d(r,t) = \frac{1}{N}\left\langle \sum_i \sum_{j\neq i} \delta[r - |\boldsymbol{r}_i(t) - \boldsymbol{r}_j(0)|] \right\rangle. \qquad (4)$$

N is the total number of particles (here 30), δ is the Dirac's function, and $\boldsymbol{r}_i(t)$ is the position vector of the ith particle (i.e., the center of mass of a dendrimer) at time t. $G_d(t)$ is proportional to the probability that a particle is at position $\boldsymbol{r}$ at time t given that a *distinct* particle was at the origin ($\boldsymbol{r} = 0$) at time $t = 0$. This function essentially probes density fluctuations arising from collective particle motions at different length- and timescales. At $t = 0$, the distinct Van Hove function is proportional to the radial distribution function $g(r)$, $G_d(r, 0) = \rho g(r)$ where ρ corresponds to the particles' density. At large timescales and sufficiently long separations, the position of each particle becomes uncorrelated to the starting position of another particle, so that $G_d(r, t)$ reaches a constant value corresponding to the average density of the particles in the system. Examples of $G_d(r, t)$ are shown in Figure 9 for the two models at the lower and the higher l_B values examined.

At low Bjerrum length and for both systems, the peak indicating the spatial correlation between nearest neighbors loses coherency (i.e., lowers its amplitude) at a rather short period of time, of the order of few tens of τ. This progressive loss of its amplitude as time lapses, arises from the collective motion of dendrimers within the complexes. At $l_B/\sigma = 10$ the main peak remains discernible for a considerably longer temporal period (about a decade longer), implying a much slower decorrelation of the relative positions between immediate neighbors and thus a longer "memory" of the original (i.e., at $t = 0$) arrangement of dendrimers.

The time period up to which the closest-neighbor maximum survives before being smeared out, can be used as a measure of the timescale related to the initial decay of the characteristic density fluctuations arising from the collective motion of the dendrimers and effectively of the formed complexes. This timescale can be estimated by monitoring the rate of decay of the main peak of $G_d(r, t)$ with respect to the amplitude at time $t = 0$, by means of the function $C(t)$

$$C(t) = \frac{G_d(r,t) - G_d(r,t^*)}{G_d(r,0) - G_d(r,t^*)}. \qquad (5)$$

$C(t)$ starts from 1 at $t = 0$ and reaches 0 at $t = t^*$, where t^* represents the timescale at which the peak corresponding to the closest neighbor shell is no longer practically discernible.

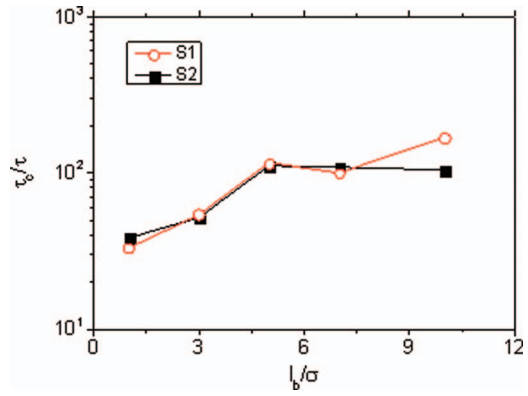

FIG. 10. Characteristic times for the decay of the collective dendrimer motion as a function of l_B for the examined systems.

Calculation of $C(t)$ was performed for both systems and for all the examined Bjerrum lengths (see Figure S10 in the supplementary material[55]). It was found that $C(t)$ could be well approximated by an exponential form, i.e., $C(t) \propto e^{-t/\tau_c}$, and thus τ_c could be taken as a characteristic time for the initial decay of $C(t)$. The exponential character of $C(t)$ indicates the absence of significant dynamic heterogeneities in the collective motion of the complexes in the probed time- and lengthscales.[103] The so-estimated times characteristic of the collective dendrimer motion are plotted in Figure 10. Following the trend shown in this plot, it appears that increase of Bjerrum length from $l_B/\sigma = 1$ to $l_B/\sigma = 5$ imparts a slowing down in the collective dendrimer motion by approximately a factor of 5, whereas at higher levels of electrostatic interactions the corresponding times show a much weaker dependence on l_B.

This picture differentiates the behavior of the present models at the examined timescales, from a typical colloidal glass-forming system,[97,104,105] since at the latter case a power-law increase of the structural relaxation time is to be expected when approaching the glassy state (note, however, that in this case this power-law divergence may refer to lengthscales much larger compared to the size of a single colloidal particle). In the present case, the timescale for the initial decay of the fluctuations of the average density due to the dendrimer motion within the polymer-rich region remains almost constant as soon as the supramolecular pattern of the complexes is well established.

Knowledge of the aforementioned timescale which describes the average density fluctuations associated with the dendrimer/LPE complexes at early times becomes important when it comes to the responsiveness of the supramolecular structure to changes in the conditions of the local environment. In addition, in the more general context of polyelectrolyte systems where self-assembly phenomena take place, the timescale related to the dynamic response of the counterions can be a key parameter towards a better understanding of the morphological characteristics of the complexes, since the ionic atmosphere formed in the vicinity of the polyelectrolytes might affect their conformational properties.[106,107] Even more so in the present case, where the stimuli for complex formation arises from the variation of the intensity of electrostatic interactions. Since the effective charge profiles of the complexes can be affected by the presence of the physically bound counterions (see Figure 4), while in principle the flexibility of the charged linear chains–and thus the realization of certain conformational states–may depend on the longevity of the formed monomer/counterion pairs, it is of interest to examine the timescales related to the survival of the transient ionic pairs between the charged monomers and the respective counterions. To this end, we have monitored the residence time of the counterions located close to charged polymer beads through the calculation of the "survival time" correlation function defined as

$$S(t) = \frac{\sum_{(i,j)} p_{ij}(t)}{\sum_{(i,j)} p_{ij}(t=0)}. \quad (6)$$

Here, $p_{ij}(t)$ assumes a value of 1 if a pair between a counterion (denoted by an index i) and a charge monomer (assigned an index j) that exists at $t = 0$ survives at time $t > 0$, and 0 otherwise. A charged monomer and a counterion are counted as an electrostatic pair at time t, if their distance at that time remains shorter than the separation denoted by the first minimum of the corresponding pair distribution functions. For all the examined systems, this minimum was approximately $r_{pair} \cong 1.6\sigma$ (see Figure S6 in the supplementary material[55]). It should be noted here that this definition of residence time (usually referred to as "intermittent" time[108]) does not take into account the rapid breaking/reformation occurrences of the electrostatic pairs that can take place within this time period, since we are interested in the average time span in which the counterions remain at the close vicinity of

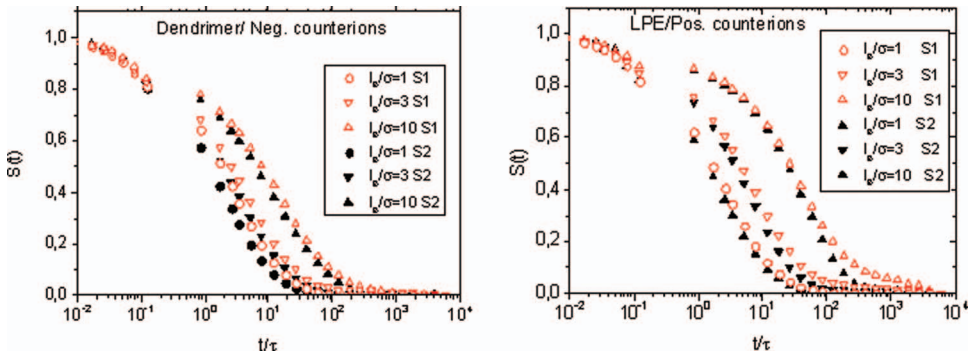

FIG. 11. Survival correlation functions for the pairs between charged polymer beads and the respective counterions at different Bjerrum lengths. Curves for $l_B/\sigma = 5$ and $l_B/\sigma = 7$ are not shown to avoid congestion.

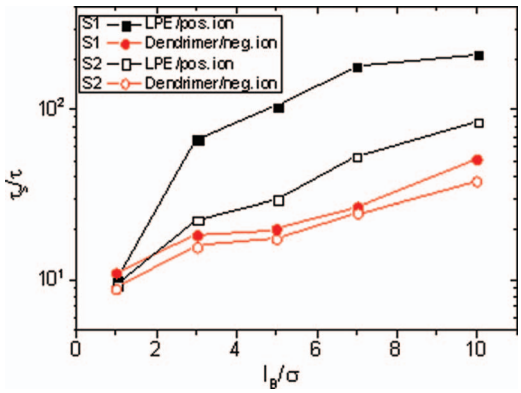

FIG. 12. Comparison of the survival times of the different electrostatic pairs between charged monomers and the corresponding counterions.

the oppositely charged monomers even if their distance may instantly surpass the considered separation limit r_{pair}.

An average survival time τ_s can be estimated by integrating the relevant correlation function, i.e., $\tau_s = \int_0^\infty S(t)dt$. We have performed this calculation for all such electrostatic pairs and for all the examined l_B values (see Figure S11 in the supplementary material[55]). Figure 11 presents examples of such correlation functions. A common attribute describing the behavior of $S(t)$ for both systems is that by increasing the intensity of electrostatic interactions the correlation functions decay at longer times. This behavior is anticipated since a higher level of electrostatic interactions would prolong the time interval for which the two oppositely charged moieties stay at a close proximity.

A distinct feature between spectra of the two different models is that at the system comprised by the shorter LPE chains the survival functions decorrelate at longer timescales. To quantify such differences between the various monomer/counterion pairs, we calculated the average residence times τ_s and compared them in Figure 12. As expected, τ_s shows a trend to increase as the strength of electrostatic interactions grows. The relevant timescales vary from about 10τ to more than 100τ depending on the system and on the strength of electrostatic interactions.

In both systems the dendrimer/counterion pairs exhibit a residence time much shorter compared to that corresponding to the LPE/counterion analogues. This behavior can be correlated to the lower degree of counterion condensation that was observed on the dendritic components (see Figure S7 in the supplementary material[55]). It is also remarkable that the LPE/counterion pairs last considerably longer in S1 (almost 5 times as much) compared to those formed in the longer LPE system, implying also counterion-related different entropic contributions to the free energy among the two systems. A comparison of the relevant timescales with that describing the timescale of the initial decay of the density fluctuations due to the motion of the dendrimer/LPE complexes (Figure 10), reveals that in the non-stoichiometric system the corresponding residence time remains well below this range and thus can be coupled to faster dynamic modes of the linear polyelectrolyte, such as more localized conformational changes. A factor of 5 between the aforementioned timescales should in principle be detectable by dielectric and birefringence experiments probing the high frequency (commonly termed as "HF") ionic motion in polyelectrolyte solutions.[109] In this case, the above description may serve as the basis for the explanation of the origin of possible differences in the ionic transport between systems of different LPE lengths.

V. SUMMARY/CONCLUSIONS

In this work, we have examined multi-molecular mixtures comprised by peripherally charged dendrimers and oppositely charged linear polyelectrolytes with explicit solvent and counterions. We have explored the effects of varying the strength of electrostatic interactions from low to moderate levels, in the structural and dynamic response of two systems comprised by linear chains differing by a factor of 2 in their monomer number, which resulted to 1.2 and 1.8 times larger radius of gyration values with respect to those of the dendtritic components. To avoid jamming effects[75] at lower strengths of electrostatic interactions, we have kept the total volume fraction well below the overlap concentration of the polymeric components, while the dimensions of the simulation box was more than ten times larger than the average size of the dendrimers and more than 7 times larger compared to the average size of the longer LPE chains.

We have found that under such conditions, for both systems increase of the strength of electrostatic interactions resulted in the formation of film-like supramolecular assemblies in the polymer-rich region, with well-defined structural patterns characterized by spatial heterogeneities at nanoscale dimensions. The morphological details of the formed structures at a lengthscale comparable to the size of a dendrimer depended upon the size of the linear polyelectrolyte, via the realization of distinct LPE conformations determined by the interplay between energetic and entropic factors. These distinct interconnection possibilities between the complexes depending on the size of the linear chain may offer a route towards a fine control of the mechanical properties of such nanoassemblies.

Moreover, it was found that due to the preferential binding of the LPEs with the dendrimer molecules, a local charge reversal close to the dendrimer periphery was observed already from a rather low level of electrostatic interactions. The absolute value of the effective charge near the boundaries of the dendrimer molecules appear to increase as the Coulombic interaction became stronger, providing thus a means of controlling the effective charge of the polymeric phase.

The approach of the formed complexes to an apparent dynamically arrested state as the Coulombic forces increased in magnitude was characterized by a gradual slow-down of different degrees of freedom of the polymeric constituents. The rotational motion of the dendritic components relaxed at different rates depending on the length of the linear polymer. This observation can be rationalized if we take into account that the realization of distinct conformations of the latter affected the geometric as well as the energetic constrictions experienced by the dendritic molecules.

The timescale associated with the early stages of the decorrelation of the density fluctuations emerging from the motion of the formed complexes, as monitored through the collective dynamics of the dendrimer components, initially increased with the intensity of electrostatic interactions and showed a trend to level-off at higher electrostatic strengths.

On the other hand, the dynamic response of the physically adsorbed positive and negative counterions exhibited different behaviors depending on the kind of the neutralizing polymeric component (i.e., dendrimer or linear chain) as well as the size of the LPE chain. The timescale describing the longevity of the pairs formed by the negative counterions and the charged dendrimer monomers, increased as the Coulombic interactions grew stronger and showed only a weak dependence on the LPE length. The corresponding residence times of the counterions bound to the linear chains, increased as well upon increasing the strength of electrostatic interactions, but the relevant timescale was differentiated significantly depending upon the length of the LPE. The pairs between the positive counterions and the shorter LPE outlived the analogous pairs formed in the twice longer LPE system by approximately a factor of 5, reaching–at high electrostatic intensities–a timescale close to that describing the collective density fluctuations of the complexes. This finding implies that properties associated with ionic transport in such systems (e.g., conductivity) can be altered by appropriate changes in the length of the LPE.

Since systems such as those studied in the present work are rather complex in nature including explicit solvent, counterions, and charged polymeric components with many degrees of freedom, the relevant parameter space associated with their thermodynamic behavior is rather broad. Among the vast number of possible combinations of features like the length of the LPEs, the size of the dendrimers, the concentration, the valency of the counterions etc., we have opted in selecting parameters which would describe systems with commonly met characteristics in the prospect of facilitating their future experimental realization (i.e., monovalent counterions, peripherally charged cationic dendrimers of the third generation, Bjerrum lengths that are experimentally realizable, anionic LPEs bearing a uniform linear charge density and with sizes comparable to the average dendrimer size). It should however be expected, that different combinations of the above parameters such as the inclusion of implicit instead of explicit solvent in the presence of strong electrostatic interactions, the use of multivalent counterions, the realization at much different concentrations or at different ionic strengths, or use of different charge densities of the polymeric components (among other parameters), might have resulted to different self-assembly characteristics than those described here.

In the context discussed above, however, we believe that the findings of the present work provides new insight in the study of mixtures comprised by linear and soft-colloidal polyelectrolytes, revealing details regarding the microscopic mechanisms related to important aspects of their physical behavior. Such information may prove useful in the design of conducting nanogels with desired properties.

ACKNOWLEDGMENTS

The present work was performed in the framework of the ESF COST action TD0802.

[1] A. M. Lowman, T. D. Dziubla, P. Bures, and N. A. Peppas, Adv. Chem. Eng. **29**, 75 (2004).
[2] C. F. Zukoski, Chem. Eng. Sci. **50**, 4073 (1995).
[3] Y. Sasaki and K. Akiyoshi, Chem. Rec. **10**, 366 (2010).
[4] C. Yi, Z. Xu, and W. T. Ford, Colloid Polymer Sci. **282**, 1054 (2004).
[5] V. Prasad, *Physics* (Harvard University Press, Cambridge, 2002), p. 120.
[6] M. Peláez-Fernández, A. Moncho-Jordá, and J. Callejas-Fernández, EPL **90**, 46005 (2010).
[7] M. Skepö and P. Linse, Macromolecules **36**, 508 (2003).
[8] T. Ohtsuka, C. P. Royall, and H. Tanaka, EPL **84**, 46002 (2008).
[9] E. Stiakakis, D. Vlassopoulos, C. N. Likos, J. Roovers, and G. Meier, Phys. Rev. Lett. **89**, 208302 (2002).
[10] H. Zhang, J. Ray, G. S. Manning, C. N. Moorefield, G. R. Newkome, and P. L. Dubin, J. Phys. Chem. B **103**, 2347 (1999).
[11] T. Radeva, V. Milkova, and I. Petkanchin, J. Colloid Interface Sci. **244**, 24 (2001).
[12] M. Pelaez-Fernandez, A. Moncho-Jorda, and J. Callejas-Fernandez, J. Chem. Phys. **134**, 054905 (2011).
[13] A. J. Khopade and F. Caruso, Nano Lett. **2**, 415 (2002).
[14] C. Li, K. Mitamura, and T. Imae, Macromolecules **36**, 9957 (2003).
[15] R. R. Netz, Phys. Rev. Lett. **90**, 128104 (2003).
[16] D. Leisner and T. Imae, J. Phys. Chem. B **108**, 1798 (2004).
[17] Y. Osada and J.-P. Gong, Adv. Mater. **10**, 827 (1998).
[18] K. Krohne, S. Duschner, D. Storkle, M. Schmidt, and M. Maskos, Macromolecules **43**, 8645 (2010).
[19] J. D. Debord, S. Eustis, S. Byul Debord, M. T. Lofye, and L. A. Lyon, Adv. Mater. **14**, 658 (2002).
[20] B. Lonetti, M. Camargo, J. Stellbrink, C. N. Likos, E. Zaccarelli, L. Willner, P. Lindner, and D. Richter, Phys. Rev. Lett. **106**, 228301 (2011).
[21] T. Dotera, J. Polym. Sci., Part B: Polym. Phys. **50**, 155 (2012).
[22] R. M. Versteegen, D. J. M. van Beek, R. P. Sijbesma, D. Vlassopoulos, G. Fytas, and E. W. Meijer, J. Am. Chem. Soc. **127**, 13862 (2005).
[23] S. V. Larin, A. A. Darinskii, E. B. Zhulina, and O. V. Borisov, Langmuir **25**, 1915 (2009).
[24] L. T. Yan and X. J. Zhang, Langmuir **25**, 3808 (2009).
[25] S. V. Larin, D. V. Pergushov, Y. Xu, A. A. Darinskii, A. B. Zezin, A. H. E. Muller, and O. V. Borisov, Soft Matter **5**, 4938 (2009).
[26] Y. Li, P. L. Dubin, R. Spindler, and D. A. Tomalia, Macromolecules **28**, 8426 (1995).
[27] C. Y. Wang, B. Y. Ren, Z. Tong, F. Zeng, X. X. Liu, S. Z. Wu, and P. Liu, Eur. Polym. J. **41**, 185 (2005).
[28] D. Leisner and T. Imae, J. Phys. Chem. B **107**, 13158 (2003).
[29] H.-L. Fu, Y.-Q. Li, L. Shao, S.-X. Cheng, X.-Z. Zhang, and R.-X. Zhuo, J. Microencapsul. **27**, 345 (2010).
[30] H. J. Yoon and W. D. Jang, J. Mater. Chem. **20**, 211 (2010).
[31] K. Gardikis, S. Hatziantoniou, M. Bucos, D. Fessas, M. Signorelli, T. Felekis, M. Zervou, C. G. Screttas, B. R. Steele, M. Ionov, M. Micha-Screttas, B. Klajnert, M. Bryszewska, and C. Demetzos, J. Pharma. Sci. **99**, 3561 (2010).
[32] H. Wang, C. Yang, L. Wang, D. Kong, Y. Zhang, and Z. Yang, Chem. Commun. **47**, 4439 (2011).
[33] S. H. M. Söntjens, D. L. Nettles, M. A. Carnahan, L. A. Setton, and M. W. Grinstaff, Biomacromolecules **7**, 310 (2006).
[34] J. M. Criscione, B. L. Le, E. Stern, M. Brennan, C. Rahner, X. Papademetris, and T. M. Fahmy, Biomaterials **30**, 3946 (2009).
[35] A. Mitra and T. Imae, Biomacromolecules **5**, 69 (2004).
[36] D. H. Zhang, P. D. Hamilton, J. L. F. Kao, S. Venkataraman, K. L. Wooley, and N. Ravi, J. Polym. Sci., Polym. Chem. **45**, 2569 (2007).
[37] N. K. Jain and U. Gupta, Expert Opin. Drug Metabol. Toxicol. **4**, 1035 (2008).
[38] J. Khandare, M. Calderon, N. M. Dagia, and R. Haag, Chem. Soc. Rev. **41**, 2824 (2012).
[39] T. Garg, O. Singh, S. Arora, and R. Murthy, Int. J. Pharma. Sci. Res. **7**, 211 (2011).
[40] T. Dutta, N. K. Jain, N. A. J. McMillan, and H. S. Parekh, Nanomed. Nanotechnol. Biol. Med. **6**, 25 (2010).
[41] H. L. Fu, S. X. Cheng, X. Z. Zhang, and R. X. Zhuo, J. Gene Med. **10**, 1334 (2008).

[42]C. Dufes, I. F. Uchegbu, and A. G. Schatzlein, Adv. Drug Delivery Rev. **57**, 2177 (2005).
[43]J. D. Eichman, A. U. Bielinska, J. F. Kukowska-Latallo, and J. R. Baker, Pharm. Sci. Technol. Today **3**, 232 (2000).
[44]X. Liu, C. Liu, E. Laurini, P. Posocco, S. Pricl, F. Qu, P. Rocchi, and L. Peng, Mol. Pharm. **9**, 470 (2011).
[45]T. Imae and A. Miura, J. Phys. Chem. B **107**, 8088 (2003).
[46]V. A. Kabanov, V. G. Sergeyev, O. A. Pyshkina, A. A. Zinchenko, A. B. Zezin, J. G. H. Joosten, J. Brackman, and K. Yoshikawa, Macromolecules **33**, 9587 (2000).
[47]J. T. Zhang, S. W. Huang, and R. X. Zhuo, Macromol. Biosci. **4**, 575 (2004).
[48]W. D. Tian and Y. Q. Ma, Macromolecules **43**, 1575 (2010).
[49]S. V. Lyulin, I. Vattulainen, and A. A. Gurtovenko, Macromolecules **41**, 4961 (2008).
[50]J. S. Klos and J. U. Sommer, J. Chem. Phys. **134**, 204902 (2011).
[51]S. V. Larin, A. A. Darinskii, A. V. Lyulin, and S. V. Lyulin, J. Phys. Chem. B **114**, 2910 (2010).
[52]G. Dalakoglou, K. Karatasos, S. Lyulin, S. Larin, A. Darinskii, and A. Lyulin, Polymers **4**, 240 (2012).
[53]S. V. Lyulin, K. Karatasos, A. Darinskii, S. Larin, and A. V. Lyulin, Soft Matter **4**, 453 (2008).
[54]G. K. Dalakoglou, K. Karatasos, S. V. Lyulin, and A. V. Lyulin, J. Chem. Phys. **127**, 214903 (2007).
[55]See supplementary material at http://dx.doi.org/10.1063/1.4757666 for Figures S1–S11.
[56]K. Karatasos, Macromolecules **41**, 1025 (2008).
[57]K. Karatasos and M. Krystallis, J. Chem. Phys. **130**, 114903 (2009).
[58]K. Karatasos and I. Tanis, Macromolecules **44**, 6605 (2011).
[59]S. L. Mayo, B. D. Olafson, and W. A. Goddard III, J. Phys. Chem. **94**, 8897 (1990).
[60]J. D. Weeks, D. Chandler, and H. C. Anderson, J. Chem. Phys. **54**, 5237 (1971).
[61]P. K. Maiti, T. Cagin, B. Wang, and W. A. Goddard III, Macromolecules **37**, 6236 (2004).
[62]F. Tarazona-Vasquez and P. B. Balbuena, J. Phys. Chem. B **109**, 12480 (2005).
[63]N. Zacharopoulos and L. G. Economou, Macromolecules **35**, 1814 (2002).
[64]G. K. Dalakoglou, K. Karatasos, S. V. Lyulin, and A. V. Lyulin, Mater. Sci. Eng., B **152**, 114 (2008).
[65]A. A. Gurtovenko, S. V. Lyulin, M. Karttunen, and I. Vattulainen, J. Chem. Phys. **124**, 094904 (2006).
[66]D. E. Galperin, V. A. Ivanov, M. A. Mazo, and A. R. Khokhlov, Polym. Sci., Ser. A **47**, 61 (2005).
[67]M. E. Leunissen, C. G. Christova, A.-P. Hynninen, C. P. Royall, A. I. Campbell, A. Imhov, M. Dijkstra, R. van Roij, and A. van Blaaderen, Nature (London) **437**, 235 (2005).
[68]A. Yethiraj and A. van Blaaderen, Nature (London) **421**, 6922 (2003).
[69]A. Bonincontro, C. Cametti, B. Nardiello, S. Marchetti, and G. Onori, Biophys. Chem. **121**, 7 (2006).
[70]Y. H. Niu and R. A. Crooks, Chem. Mater. **15**, 3463 (2003).
[71]M. Liu and J. M. J. Fréchet, Polym. Bull. **43**, 379 (1999).
[72]G. Nisato, R. Ivkov, and E. J. Amis, Macromolecules **33**, 4172 (2000).
[73]W.-d. Tian and Y.-q. Ma, J. Phys. Chem. B **113**, 13161 (2009).
[74]P. G. Ferreira, M. Dymitrowska, and L. Belloni, J. Chem. Phys. **113**, 9849 (2000).
[75]K. Karatasos and M. Krystallis, Macromol. Symp. **278**, 32 (2009).
[76]L. T. Yan and X. J. Zhang, Soft Matter **5**, 2101 (2009).
[77]Z. Y. Ou and M. Muthukumar, J. Chem. Phys. **124**, 154902 (2006).
[78]I. I. Potemkin, Europhys. Lett. **68**, 487 (2004).
[79]S. Pietronave, L. Arcesi, C. D'Arrigo, and A. Perico, J. Phys. Chem. B **112**, 15991 (2008).
[80]A. E. Larsen and D. G. Grier, Nature (London) **385**, 230 (1997).
[81]T. E. Angelini, R. Golestanian, R. H. Coridan, J. C. Butler, A. Beraud, M. Krisch, H. Sinn, K. S. Schweizer, and G. C. L. Wong, Proc. Natl. Acad. Sci. U.S.A. **103**, 7962 (2006).
[82]E. Allahyarov, I. D'Amico, and H. Lowen, Phys. Rev. Lett. **81**, 1334 (1998).
[83]J. Wu, D. Bratko, and J. M. Prausnitz, Proc. Natl. Acad. Sci. U.S.A. **95**, 15169 (1998).
[84]A. J. Khopade and F. Caruso, Langmuir **18**, 7669 (2002).
[85]M. Ujihara and T. Imae, Polym. Int. **59**, 137 (2010).
[86]M. J. Stevens, Phys. Rev. Lett. **82**, 101 (1999).
[87]Y. De-Wei, Y. Qiliang, and J. J. de Pablo, J. Chem. Phys. **123**, 174909 (2005).
[88]T. Terao, Chem. Phys. Lett. **446**, 350 (2007).
[89]V. N. Bliznyuk, F. Rinderspacher, and V. V. Tsukruk, Polymer **39**, 5249 (1998).
[90]C. Mayer, E. Zaccarelli, E. Stiakakis, C. N. Likos, F. Sciortino, A. Munam, M. Gauthier, N. Hadjichristidis, H. Iatrou, P. Tartaglia, H. Lowen, and D. Vlassopoulos, Nature Mater. **7**, 780 (2008).
[91]L. Angelani, G. Foffi, F. Sciortino, and P. Tartaglia, J. Phys.: Condens. Matter **17**, L113 (2005).
[92]T. M. Hermans, M. A. C. Broeren, N. Gomopoulos, P. van der Schoot, M. H. P. van Genderen, N. A. J. M. Sommerdijk, G. Fytas, and E. W. Meijer, Nat. Nanotechnol. **4**, 721 (2009).
[93]K. A. Dawson, Curr. Opin. Colloid Interface Sci. **7**, 218 (2002).
[94]M. L. Kilfoil, E. E. Pashkovski, J. A. Masters, and D. A. Weitz, Philos. Trans. R. Soc. London **361**, 753 (2003).
[95]E. K. Hobbie and A. D. Stewart, Phys. Rev. E **61**, 5540 (2000).
[96]G. Foffi, F. Sciortino, P. Tartaglia, E. Zaccarelli, F. Lo Verso, L. Reatto, K. A. Dawson, and C. N. Likos, Phys. Rev. Lett. **90**, 238301 (2003).
[97]P. N. Segre, V. Prasad, A. B. Schofield, and D. A. Weitz, Phys. Rev. Lett. **86**, 6042 (2001).
[98]S. Manley, L. Cipelletti, V. Trappe, A. E. Bailey, R. J. Christianson, U. Gasser, V. Prasad, P. N. Segre, M. P. Doherty, S. Sankaran, A. L. Jankovsky, B. Shiley, J. Bowen, J. Eggers, C. Kurta, T. Lorik, and D. A. Weitz, Phys. Rev. Lett. **93**, 108302 (2004).
[99]M. Tokuyama, Phys. Rev. E **58**, R2729 (1998).
[100]K. Karatasos, D. B. Adolf, and G. R. Davies, J. Chem. Phys. **115**, 5310 (2001).
[101]E. R. Weeks, J. C. Crocker, A. C. Levitt, A. B. Schofield, and D. A. Weitz, Science **287**, 627 (2000).
[102]R. Zangi and S. A. Rice, Phys. Rev. E **68**, 061508 (2003).
[103]M. Laurati, G. Petekidis, N. Koumakis, F. Cardinaux, A. B. Schofield, J. M. Brader, M. Fuchs, and S. U. Egelhaaf, J. Chem. Phys. **130**, 134907 (2009).
[104]S. Sanyal and A. K. Sood, Phys. Rev. E **57**, 908 (1998).
[105]R. Zorn and U. Buchenau, *Glass Transition in Colloids and Undercooled Liquids* (Springer, Berlin, 2005), p. 125.
[106]T. E. Angelini, H. Liang, W. Wriggers, and G. C. L. Wong, Proc. Natl. Acad. Sci. U.S.A. **100**, 8634 (2003).
[107]T. S. Lo, B. Khusid, and J. Koplik, Phys. Rev. Lett. **100**, 128301 (2008).
[108]A. Luzar, J. Chem. Phys. **113**, 10663 (2000).
[109]J. Oizumi, Y. Kimura, K. Ito, and R. Hayakawa, Colloid Surf., A **145**, 101 (1998).